

Simulation of the Phase Behavior of the (EO)₁₃(PO)₃₀(EO)₁₃(Pluronic L64)/Water/*p*-Xylene System Using MesoDyn

S. L. Guo, T. J. Hou, and X. J. Xu*

College of Chemistry and Molecular Engineering, Peking University,
Beijing 100871, People's Republic of China

Received: June 16, 2002; In Final Form: August 26, 2002

The phase behavior of the (EO)₁₃(PO)₃₀(EO)₁₃(Pluronic L64)/water/*p*-xylene system in the mesoscopic region was investigated using MesoDyn, a new dynamic density functional method. The “equivalent chain” method was used to perform the parametrization of the Gaussian chain. In this paper, we compare the mesoscopic morphology formations of systems at different concentrations of solvents and discuss the effect of water on the formation of micelles. The calculated results show that Pluronic L64 does not form polymolecular micelles in pure *p*-xylene or in the presence of a small amount of water, but with an increase in the concentration of water, polymolecular micelles in different shapes were formed. By analyzing the water distributions of the systems after 1000 simulation steps, we prove that free water does exist in the micellar core. The effects of temperature and PEO and PPO block sizes are also investigated. The results indicate that the formation of reverse micelles is exothermic, and so the formation of reverse micelles becomes more difficult and the rate becomes slower with increasing temperature. Moreover, PEO block size has a stronger effect on the formation of reverse micelles compared with that of the PPO block size.

1. Introduction

In the microscopic region, phase behavior can be modeled using a detailed molecular description, often with techniques such as molecular dynamics (MD) and Monte Carlo (MC) simulations. In the macroscopic region, phase separation models can be based on equations of state, which are fitted to macroscopic phase diagrams. In the mesoscopic region, local concentration fields can be used as collective variables to obtain a description of self-assembly structures. The mesoscopic dynamics models are receiving increasing attention as they form a bridge between fast molecular kinetics and slow thermodynamic relaxations of macroscale properties.

Pluronic (PEO–PPO–PEO block copolymer, PEO = poly(ethylene oxide), PPO = poly(propylene oxide)), one type of nonionic surfactant, is widely used in detergents, foam formations, dispersion stabilizations, lubrication, and drug delivery and has received wide attention in the literature.^{1–5} The action of Pluronic depends strongly on system morphology, which is known to include micelles that can reversibly gel, as well as on bicontinuous, hexagonal, and lamellar phases. There are several factors contributing to the morphology formation including the temperature, the solvent quality, the PEO and PPO block sizes, etc. In the past decade, much work including experiments and simulations has been done on Pluronic in aqueous solution;^{6–11} also there are a few experimental papers about Pluronic in double solvents,^{12–16} but there have been few theoretical simulations in double solvents. Taking account of the long period and the poor repeatability of the experiments, the simulation work in double solvents is very important, which must be helpful for us to further investigate this type of system. In the current work, the MesoDyn method was used to simulate

the (EO)₁₃(PO)₃₀(EO)₁₃(Pluronic L64)/water/*p*-xylene system. The influences of the temperature, the PEO and PPO block sizes, and the concentrations of two solvents were investigated systematically.

2. Method

The basic idea in the MesoDyn method is the density functional theory. It is based on the idea that the free energy F of an inhomogeneous liquid is a function of the local density function ρ . From the free energy, all thermodynamic functions can be derived so that for instance phase transitions can be investigated as a function of the density distribution in the system.

In MesoDyn, the method used to model the time evolution of a mesoscopic system is the time-dependent Ginzburg–Landau model. Ginzburg–Landau models generally consist of a phenomenological expansion of the free energy in the density, which is used to model thermodynamic forces and a set of stochastic diffusion or modified Navier–Stokes equations to predict the time evolution. The numerical calculation involves the integration of functional Langevin equations, given an implicit inverse Gaussian density functional expression for the intrinsic chemical potentials. Local nonideal interactions are included via a mean field. Mesoscopic fluctuations are introduced by the explicit inclusion of noise sources according to the fluctuation–dissipation theorem. Work on coarse-grained time-dependent Ginzburg–Landau models can be found in refs 17–21. For a detailed description of the theory of the MesoDyn, see ref 22.

On a coarse-grained time scale, $\rho_1^0(r)$ is defined as a collective concentration field of the beads of type I at an instant in time and serve as a reference level. There will be a certain distribution of bead positions, defined as $\Psi(R_{11}, \dots, R_{nN})$, where $R_{\gamma s}$ is the position of a bead s from chain γ . Given the

* To whom correspondence should be addressed. E-mail: xiaojxu@chem.pku.edu.cn.

distribution Ψ , we can define the collective concentration of beads s from all chains by the average of a microscopic density operator:

$$\rho_I[\Psi](r) \equiv \sum_{\gamma=1}^n \sum_{s=1}^N \delta_{Is}^K Tr \Psi \delta(r - R_{\gamma s}) \quad (1)$$

where δ_{Is}^K is the Kronecker function with a value of 1 when bead s is of type I and 0 otherwise. It is assumed that in the slowly relaxing liquid the interactions do not depend on the momenta.

We can define a set of distribution functions Ψ with the constraint $\rho_I[\Psi](r) = \rho_I^0(r)$:

$$\Omega = \{\Psi(R_{11}, \dots, R_{nN}) | \rho_I[\Psi](r) = \rho_I^0(r)\} \quad (2)$$

All distributions Ψ of the set Ω lead to the same density $\rho_I^0(r)$. On the basis of this set of distribution functions, an intrinsic free-energy functional $F[\Psi]$ can be defined:

$$F[\Psi] = Tr(\Psi H^{id} + \beta^{-1} \Psi \ln \Psi) + F^{nid}[\rho^0] \quad (3)$$

The first term is the average value of the Hamiltonian for internal Gaussian chain interactions.^{23,24} The second term in the free-energy functional represents the Gibbs entropy of the distribution $-k_B T \Psi \ln \Psi$. The third term $F^{nid}[\rho^0]$ is the mean-field nonideal contribution.

The key rudiment of dynamic density functional theory is that now on a coarse-grained time scale the distribution function Ψ is such that the free-energy functional $F[\Psi]$ is minimized. Hence, Ψ is independent of the history of the system and is fully characterized by the constraints that it represents the density distribution and minimizes the free-energy functional. This constraint on the density fields is realized by means of an external potential U_I .

The constraint minimization of the free-energy functional leads to an optimal distribution, which in turn, and by the one-to-one relation between densities, distributions, and external potential, can be written as

$$\beta F[\rho] = n \ln \Phi + \beta^{-1} \ln n! - \sum_I \int U_I(r) \rho_I(r) dr + \beta F^{nid}[\rho] \quad (4)$$

Finally, a Flory–Huggins-type interaction is introduced for the nonideal (interchain) interactions:

$$F^{nid}[\rho] = \frac{1}{2} \int \int \epsilon_{AA}(|r - r'|) \rho_A(r) \rho_A(r') + \epsilon_{AB}(|r - r'|) \rho_A(r) \rho_B(r') + \epsilon_{BA}(|r - r'|) \rho_B(r) \rho_A(r') + \epsilon_{BB}(|r - r'|) \rho_B(r) \rho_B(r') dr dr' \quad (5)$$

where $\epsilon_{IJ}(|r - r'|)$ is a mean-field energetic interaction between beads of type I at r and type J at r' .

The mean-field intrinsic chemical potentials can easily be derived by functional differentiation of the free energy: $\mu_I(r) = \delta F / \delta \rho_I(r)$. At equilibrium, $\mu_I(r) = \text{constant}$, which results in the familiar self-consistent-field equations for the mean-field Gaussian chain model. In general, these equations will have many solutions, one of which will be a state of lowest free energy; most states will be metastable. When the system is not in equilibrium, $-\nabla \mu_I(r)$ is a thermodynamic force that by the inversion of the density functional and the explicit form of the nonideal interactions is a unique functional of the density. On

the basis of these equations, we can set up the generalized time-dependent Ginzburg–Landau theory.

The derivation of the diffusive dynamics of the molecular ensemble is based on the assumption that for each type of bead I the local flux is proportional to the local bead concentration and the local thermodynamic driving force: $J_I = -M \rho_I \nabla \mu_I + J'_I$, where J'_I is the stochastic flux (related to thermal noise). Together with the continuity equation

$$\frac{\partial \rho_I}{\partial t} + \nabla J_I = 0 \quad (6)$$

this leads to simple diagonal-functional Langevin equations (stochastic diffusion equations) in the density fields with a Gaussian distribution of the noise:

$$\frac{\partial \rho_I}{\partial t} = M \nabla \rho_I \nabla \mu_I + \eta_I \quad (7)$$

However, the fluctuations in the total density of this simple system are not realistic because finite compressibility is not enforced by the mean-field potential chosen (see below). Therefore, total density fluctuations are simply removed by introducing an incompressibility constraint:

$$(\rho_A(\mathbf{r}, t) + \rho_B(\mathbf{r}, t)) = \frac{1}{\nu_B} \quad (8)$$

where ν_B is the average bead volume. This condition then leads to exchange Langevin equations:

$$\frac{\partial \rho_A}{\partial t} = M \nu_B \nabla \rho_A \rho_B \nabla [\mu_A - \mu_B] + \eta \quad (9)$$

$$\frac{\partial \rho_B}{\partial t} = M \nu_B \nabla \rho_A \rho_B \nabla [\mu_B - \mu_A] - \eta \quad (10)$$

Here, M is a bead mobility parameter. The kinetic coefficient $M \nu_B \rho_A \rho_B$ models a local exchange mechanism. Hence, the model is strictly valid only for Rouse dynamics.

The distribution of the Gaussian noise satisfies the fluctuation–dissipation theorem and ensures that the time integration of the Langevin equations generates an ensemble of density fields with Boltzmann distributions:

$$\langle \eta(r, t) \rangle = 0 \quad (11)$$

$$\langle \eta(r, t) \eta(r', t') \rangle = -\frac{2M \nu_B}{\beta} \delta(t - t') \nabla_r \times \delta(r - r') \rho_A \rho_B \nabla_{r'} \quad (12)$$

In the MesoDyn method, the molecules are defined on a coarse-grained level as “Gaussian chains of beads”. Each bead is of a certain component type representing covalently bonded groups of atoms such as those given by one or a few monomers of a polymer chain. Chemically specific information about the molecular ensemble enters into MesoDyn via material parameters such as the self-diffusion coefficients of the bead components, the Flory–Huggins interaction parameters, the bead sizes, and the molecular architecture (chain length, branching, etc.).

The dynamics of the system is described by a set of so-called functional Langevin equations. In simple terms, these are diffusion equations in the component densities that take account of the noise in the system. By means of numerical inversions, the evolution of the component densities is simulated, starting

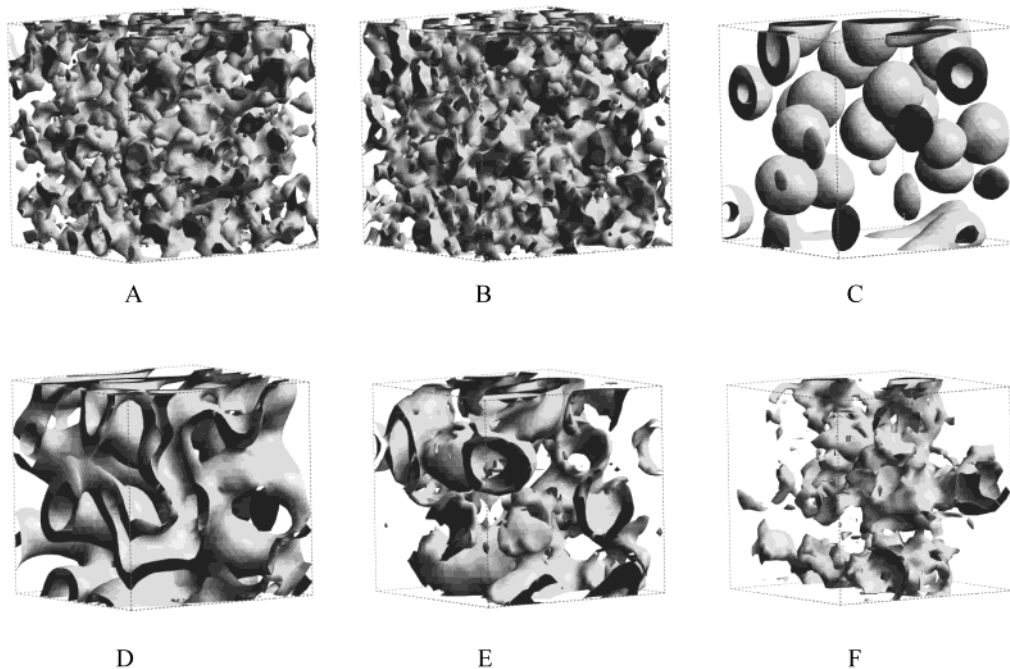


Figure 1. EO isosurface representations of six different systems after 1000 simulation steps.

from an initially homogeneous mixture in a cube of typical size 100–1000 nm and with periodic boundary conditions.

The phase behavior and phase structure of Pluronic L64/water/*p*-xylene systems, which have the same concentration of Pluronic L64 but different concentrations of solvents, have been investigated by using the MesoDyn simulation method. The influencing factors including the concentration of two solvents, temperature, and PEO and PPO block sizes were discussed. The time-evolution trajectory of the microphase separation kinetics was also discussed in detail. All the mesoscale simulations and analyses were done with the MesoDyn module in Cerius2 on a 2-CPU SGI Octane workstation.

3. Results and Discussion

Simulation Parameters. The chain of Pluronic L64 (EO)₁₃-(PO)₃₀(EO)₁₃ was defined as the Gaussian chain A₇B₁₆A₇ by the equivalent chain method.^{11,23} The bond length of the Gaussian is 8.2 Å. The dimensions of the simulation lattice used here are (32, 32, 32). The ratio of the bond length α to the length h is automatically set to $\alpha/h = 1.15430$ to ensure isotropy of all grid-restricted operators.¹⁰ To ensure a stable numerical algorithm, as an approximation, all bead volumes of types A, B, W, and X (A = PEO, B = PPO, W = H₂O, X = *p*-xylene) were 150 Å³, and all bead diffusion coefficients $D = \beta^{-1}M$ of the four types were set at $1.0 \times 10^{-7} \text{cm}^2 \text{s}^{-1}$. The simulation temperature was set at 298 K, and the time step used was 50.00 ns. The noise-scaling parameter used here was 100, and the compressibility parameter was fixed at 10.0.^{25,26}

The solvent–polymer interaction parameters were estimated as

$$\chi_{sp} = (\delta_s - \delta_p)^2 V_s / RT \quad (13)$$

where δ_s and δ_p are Scatchard–Hildebrand solubility parameters of the solvent and of the polymer, respectively,²⁷ and V_s is the molar volume of the solvent. The interaction parameters of *p*-xylene, H₂O, and PEO–PPO are not suitable to be estimated by the above equation, and consequently, χ_{wx} used here was estimated to be 5.0 because *p*-xylene is nearly insoluble in water;

TABLE 1: Interaction Parameters of Polymers and Solvents

	PPO	PEO	H ₂ O	<i>p</i> -xylene
PPO		3.0	2.1	0.03
PEO	3.0		0.3	0.5
H ₂ O	2.1	0.3		5.0
<i>p</i> -xylene	0.03	0.5	5.0	

TABLE 2: Volume Fractions of Polymer/Water/*p*-Xylene in Different Simulation Systems

system title	L64	H ₂ O	<i>p</i> -xylene
A	20	0	80
B	20	5	75
C	20	10	70
D	20	30	50
E	20	70	10
F	20	80	0

χ_{AB} was estimated by group contribution methods.^{28,29} The values for the interaction parameters of polymers and solvents are given in Table 1.

It should be noticed here that in previous papers^{11,29} χ_{Aw} and χ_{Bw} were calculated from vapor-pressure data of aqueous homopolymer solutions using the Flory–Huggins expression

$$\chi_{ij} = \theta^{-2} \{ \ln p/p^0 - \ln(1 - \theta) - (1 - 1/N)\theta \} \quad (14)$$

where p is the vapor pressure, θ is the polymer volume fraction, and N is the chain length, which is the number of monomers per bead. Calculated from the above equation, χ_{Aw} is 1.4, and χ_{Bw} is 1.7. On the basis of the solubility of PEO in water, we think these values are incorrect. Generally, when $\chi_{sp} > 0.5$, the polymer is not easily dissolved in the solvent, so $\chi_{Aw} = 1.4$ indicates that water is a poor solvent for PEO, which is clearly not in agreement with the experimental results. In our opinion, this problem may be mainly caused by the neglect of hydrogen bonding between PEO and H₂O in eq 14. This view can be confirmed by χ_{Bw} . There is much less hydrogen bonding between PPO and H₂O than between PEO and H₂O, and in this situation, the values of χ_{Bw} calculated from eq 14 agrees with experiments to some extent.

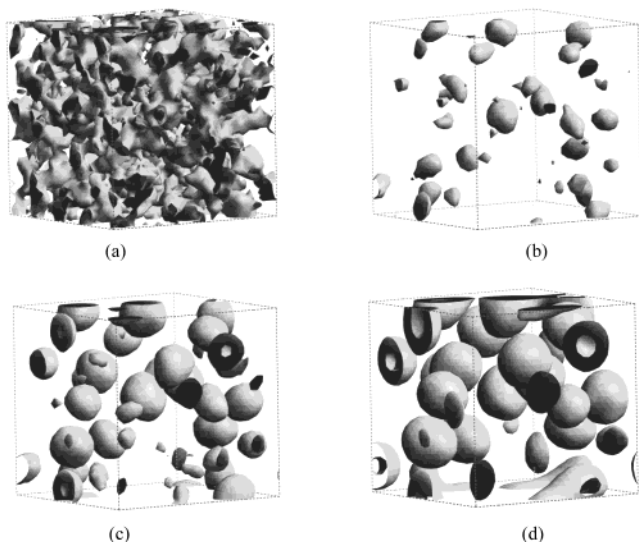


Figure 2. EO isosurface representations of the C system after different simulation steps (a–d refer to the EO isosurface representations of the C system after 100, 300, 400, and 1000 simulation steps, respectively).

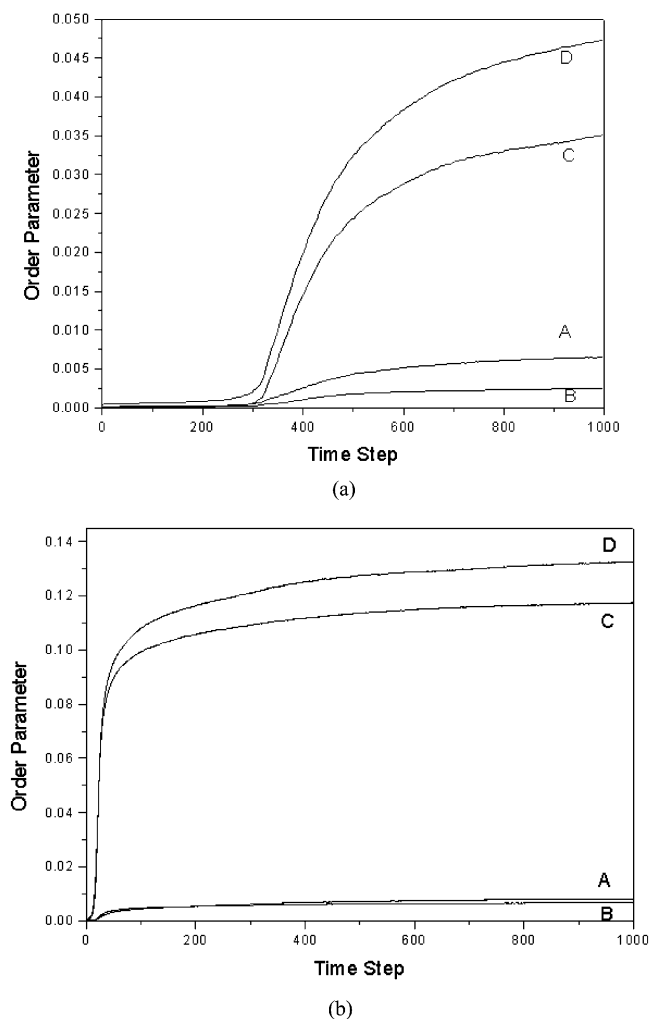


Figure 3. Time evolution of the dimensionless order parameters of the C and D systems. The labels A, B, C, and D refer to PEO, PPO, H₂O, and *p*-xylene, respectively.

Effect of Solvents. To compare the effects of solvents, simulations were performed with the same polymer concentration. The volume concentration of the polymer in all cases was

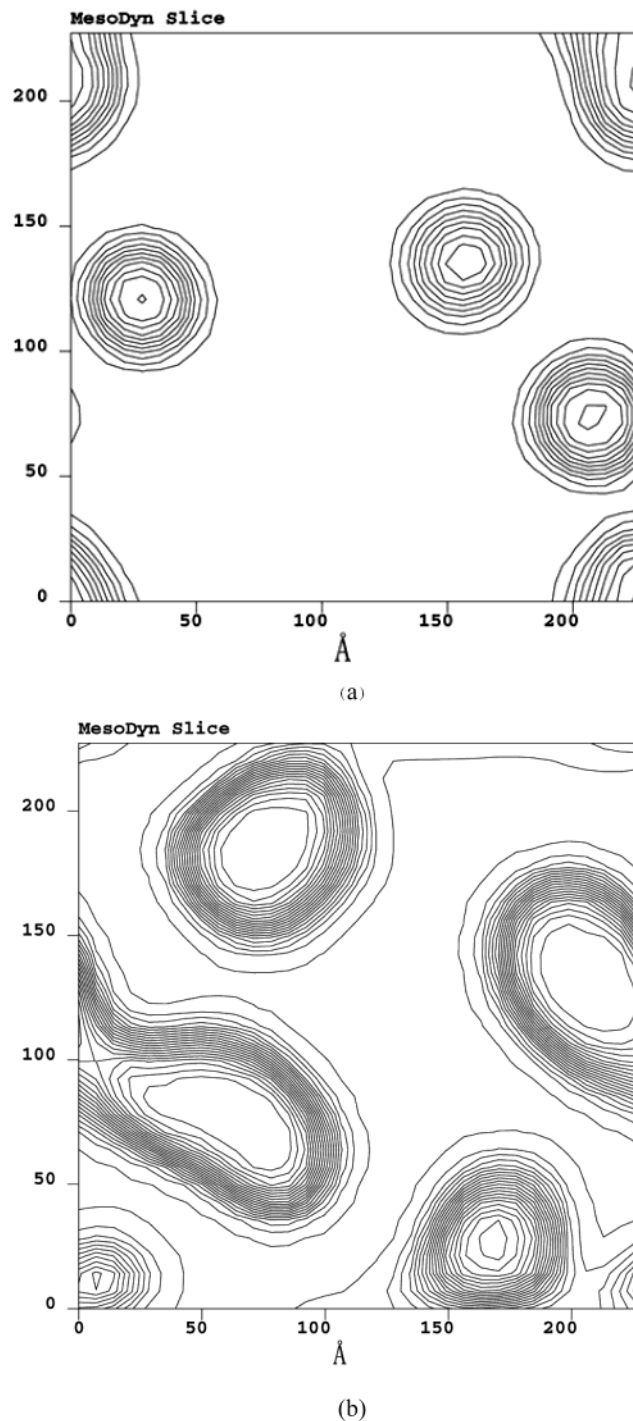


Figure 4. H₂O distribution profiles in reverse micelles of system C and D after 1000 simulation steps.

20%. Detailed concentrations for each component are given in Table 2.

The isosurfaces of EO for six different systems (see Table 2) after 1000 simulation steps at 298 K are presented in Figure 1. To clearly demonstrate the formations of systems, both isodensities of isosurfaces in Figure 1A and B are at 10%, and the other four isodensities of isosurfaces are at 15%. (Because no micelles are formed in A and B systems, the isosurfaces of isodensity at 15% for systems A and B are blank.) The formations of six systems indicate that Pluronic L64 does not form polymeric micelles in pure *p*-xylene or in the presence of a small amount of water, but with the increase in the concentration of water, polymeric micelles in different

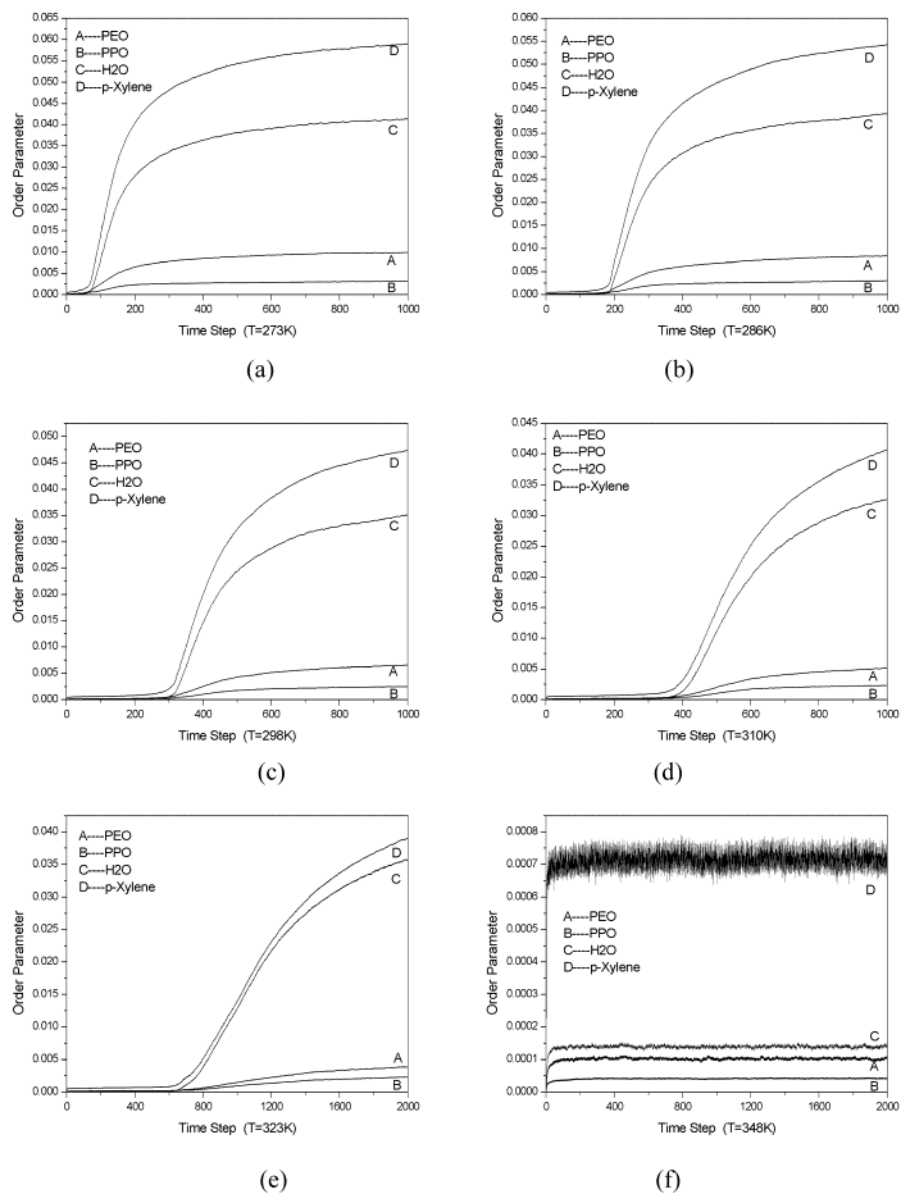


Figure 5. Time evolution of the dimensionless order parameters of six systems at different temperatures.

shapes were formed. Reverse micelles consisting of a PPO shell and a PEO and H₂O core are formed when the amount of water is small. Different concentrations of water lead to different formations of systems. When the amount of water is more than the amount of *p*-xylene, reverse micelles transfer to normal micelles, consisting of a PEO shell and a PPO and *p*-xylene core. It can be concluded that water induces the formation of micelles in the pluronic/*p*-xylene system. The simulated results are in good agreement with the experimental results qualitatively.^{12,13}

Process of Phase Behavior. To gain insight into the process of phase behavior, we carefully analyzed system C. Because system C is at the turning point of the formation of micelles in these six systems, the properties of the process of phase behavior are more characteristic than those of the other five systems. Figure 2 a–d gives the isosurface of EO of system C after 100, 300, 400, and 1000 simulation steps, respectively. All the isodensities are at 15% except in Figure 2a, which is at 10%. (Because no micelles are formed after 100 simulation steps, the isosurface of isodensity at 15% was blank.) Figure 2 shows that to some extent at the beginning of the process the solution was homogeneous and micelles were formed along with the time

evolution and that finally the solution arrived at an equilibrium state. These results also can be confirmed by the time evolution of the order parameter P of system C (Figure 3a). The dimensionless order parameter P is defined as $P = V^{-1} \int \theta_1^2(r) dr - \sum (\theta_1^0)^2$. Figure 3a indicates that the time evolution of the phase behavior can be divided into three stages. In the first, micelles were formed, and the order parameter changed slowly. In this stage, the morphology of the system varied little. Then, micelles were formed, and the order parameter ascended rapidly. In this stage, the system quickly formed the raw morphologies of micelles. This stage is quick—about 10 to 20 μ s. Finally, the system changed in a slow way to overcome the defects formed in the previous stage. This stage is time-consuming.

We investigated the order parameters of other three systems in which plenty of micelles were formed and found that these systems went through a similar process (see Figure 3b). It can be observed that in system D the process forming micelles is much shorter than that in system C; compare Figure 3 part a with part b. The only difference between system C and system D is the water concentration. It can be concluded that the amount

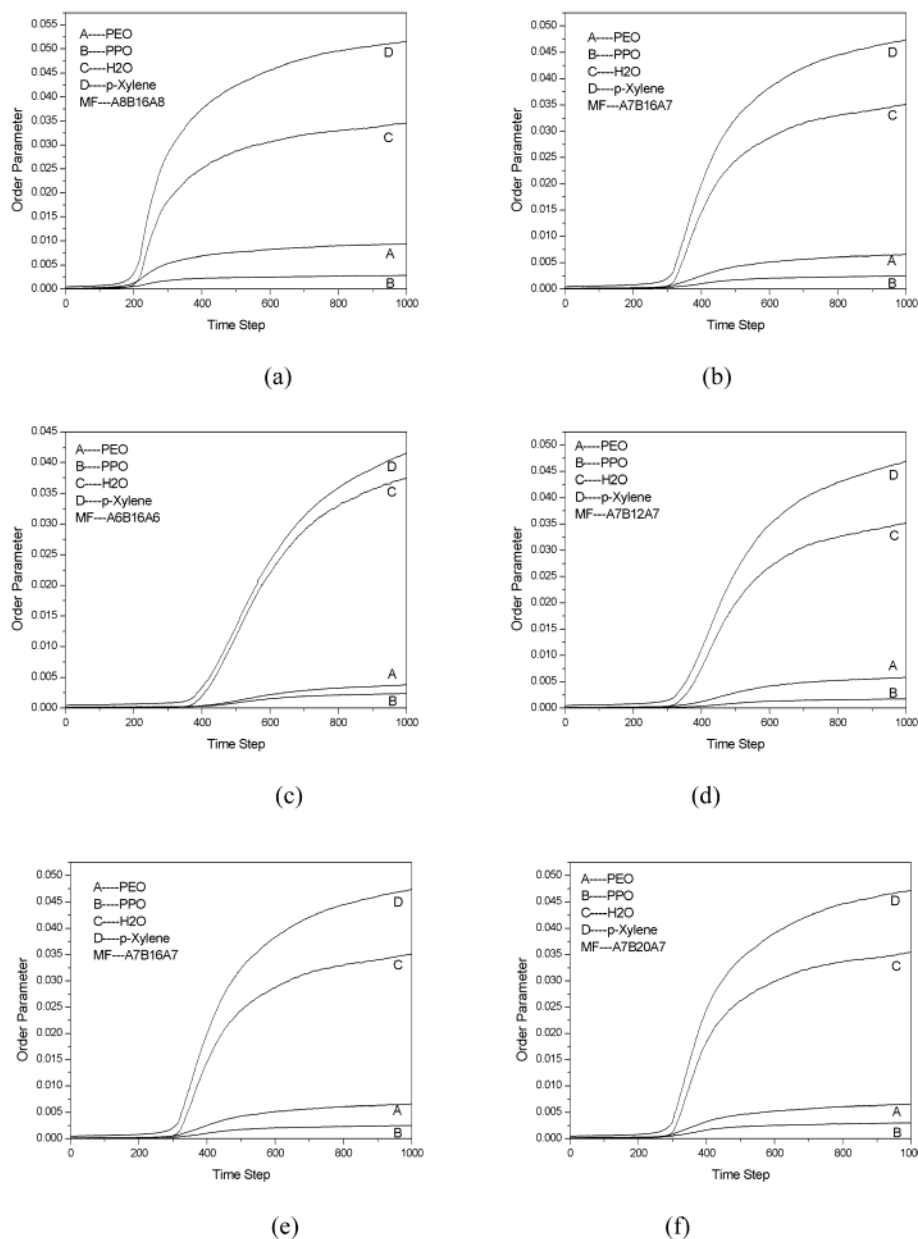


Figure 6. Time evolution of the dimensionless order parameters of different block-size systems (water in oil). a–c have different PEO block sizes but the other conditions are the same. d–e have different PPO block sizes, but the other conditions are the same.

of water influences not only the occurrence of micelles but also the rate of the formation of micelles. To our knowledge, there has been little experimental work³⁰ on water affecting the rate of formation of micelles.

Water Distribution in Reverse (Water-in-Oil) Micelle. The water distribution in the PEO–PPO–PEO/xylene/water reverse micelle has been studied by several experimental methods,³¹ but there has been no exact experimental demonstration of the water distribution in the micelle. By now, the general view is that most of the water is bound with the PEO block, evenly distributed in the core in the presence of a small amount of water; with an increase in the amount of water, there is free water in addition to the bound water in the reverse micelle.^{13,31–33} To study the water distribution in the reverse micelle, we analyzed the water distribution profiles in the reverse micelle of system C (Figure 4a) and system D (Figure 4b) after 1000 simulation steps. The closed curve in Figure 4 is the isoconcentration line of water, which represents the same concentration of water along a curve. This profile is similar to the contour map, and the concentration of water represented by the

isoconcentration line increases from the outside to the inside of the round, and finally there is a maximum value of concentration in the plateau of the round. The concentration of every point is the same in the range of the plateau. Figure 4 shows that the isoconcentration lines are closely distributed in the corona of the reverse micelle, indicating that the water is in the bound-water state in this range; the isoconcentration lines enclose a pond in the core of the reverse micelle, indicating that the water is in the free-water state in this range. The amount of water in system C (Figure 4a) just beyond the critical amount of water inducing the formation of micelles is less than that in system D (Figure 4b). On the basis of the above analyses, we can draw the conclusion that most of the water molecules are bound with the PEO block in the micelles when the amount of water is small and that the water molecules exist in the form of free water in the micelles when the amount of water increases. Our simulated results proved that free water does exist in the micellar core.

Effect of Temperature. To discuss the influence of temperature on the phase behavior, six systems (20% L64, 10% water,

70% *p*-xylene) have been simulated at different temperatures: 273, 286, 298, 310, 323, and 348 K. Figure 5a–f shows the dimensionless order parameters of six systems at different temperatures. On the basis of Figure 5 a–f, it is indicated that the temperature has a strong impact on the phase behavior of the ternary block polymer–water–oil system in addition to the water concentration. The formation of reverse micelles becomes more difficult and the rate becomes slower with increasing temperature, and even Pluronic L64 does not form reverse micelles at 348 K. This indicates that the formation of reverse micelles is exothermic. The effects of temperature on the phase behavior can be understood from the fact that PEO and PPO become more hydrophobic at increasing temperature; therefore, the solubility of PEO and PPO in water decreases, and *p*-xylene is expected to become an even better solvent for PEO and PPO, which makes the copolymers less prone to association. The experimental work of Mays gives a similar conclusion that the rate of water-in-oil microemulsions increases with decreasing temperature.³⁰ Also, the above result is in agreement with Alexandridis' experimental work³⁴ that shows that an increase in temperature makes water a worse solvent and xylene a better solvent for the copolymer and that the water solubilization capacity increases with temperature for a PEO–PPO–PEO copolymer with 40% PEO (L64 belongs to this kind of copolymer).

Effects of PEO and PPO Block Size on Phase Behavior.

The relative sizes of the hydrophilic PEO block and hydrophobic PPO block also affect the phase behavior (the formation of reverse micelles). Five systems (20% L64, 10% water, 70% *p*-xylene) under the same conditions but with different block sizes were simulated. (Figure 4b and e are the same, and this arrangement is very convenient by which to compare them.) We also analyze the dimensionless order parameters to investigate the effects of PEO and PPO block size on phase behavior. The comparison of Figure 5 part a with parts b and c shows that PEO block size has a obvious effect on phase behavior, but the comparison of Figure 5 part d with parts e and f shows that PPO block size has little influence on phase behavior. The formation of reverse micelles becomes much easier and faster with increasing PEO block size. The effect of PEO block size is similar to that of water content; it can be understood that both PEO and water belong to the polar components, which have similar properties. This simulation result agrees well with the experimental work of Alexandridis and co-workers,¹⁵ who reported that the relative size of the “solvophobic” PEO block (rather than the PPO block size) should be the controlling parameter in the tendency of the polyoxyalkylene block copolymers to form reverse micelles in organic solvents.

Conclusions

The phase behavior of the (EO)₁₃(PO)₃₀(EO)₁₃(Pluronic L 64)/water/*p*-xylene system in the mesoscopic region was successfully simulated using the MesoDyn equivalent chain method. The simulation results show that water is the key factor affecting the formation of micelles and that no micelles are formed in pure *p*-xylene or in the presence of a small amount of water but with increasing concentration of water, micelles with different shapes are largely formed. The amount of water

influences not only the occurrence of micelles but also the rate of the formation of micelles. By analyzing the water distributions of the systems after 1000 simulation steps, we found that free water did exist in the micellar core.

The influence of temperature on the phase behavior was investigated. The results show that the temperature has a strong impact on the phase behavior of the ternary block polymer–water–oil system in addition to the water concentration. The formation of reverse micelles is exothermic.

Finally, the influence of the relative sizes of the PEO and PPO blocks was investigated. The results show that the PEO block size has a bigger effect on the formation of reverse micelles compared with the PPO block size.

Acknowledgment. This project is supported by NCSF 299925902.

References and Notes

- (1) Tuzar, Z.; Kratochvil, P. *Adv. Colloid Interface Sci.* **1976**, *6*, 201.
- (2) Zhou, Z.; Chu B. *Macromolecules* **1994**, *27*, 2025.
- (3) Zhou, Z.; Chu B. *J. Colloid Interface Sci.* **1995**, *170*, 102.
- (4) Brown, W.; Schillen, K.; Almgren, M.; Hvidt, S.; Bahadur, P. *J. Phys. Chem.* **1991**, *95*, 1850.
- (5) Wanka, G.; Hoffmann, H.; Ulbricht, W. *Colloid Polym. Sci.* **1990**, *268*, 101.
- (6) Malmsten, M.; Linse, P. *Macromolecules* **1993**, *26*, 2905.
- (7) Svensson, M.; Linse, P. *Macromolecules* **1995**, *28*, 3597.
- (8) Maurits, N. M.; Fraaije, J. G. E. M. *J. Chem. Phys.* **1997**, *106*, 6730.
- (9) Maurits, N. M.; Fraaije, J. G. E. M. *J. Chem. Phys.* **1997**, *107*, 5879.
- (10) Fraaije, J. G. E. M.; Vlimmeren, B. A. C. V.; Maurits, N. M. *J. Chem. Phys.* **1997**, *106*, 4260.
- (11) Li, Y.-Y.; Hou, T.-J.; Guo, S.-L.; Xu, X.-J. *Phys. Chem. Chem. Phys.* **2000**, *2*, 2749.
- (12) Alexandridis, P.; Olsson, U. *Macromolecules* **1995**, *28*, 7700.
- (13) Wu, G.-W.; Zhou, Z.-K.; Chu, B. *Macromolecules* **1993**, *26*, 2117.
- (14) Svensson, B.; Olsson, U.; Alexandridis, P. *Langmuir* **2000**, *16*, 6839.
- (15) Alexandridis, P.; Andersson, K. *J. Phys. Chem. B* **1997**, *101*, 8103.
- (16) Alexandridis, P.; Holmqvist, P.; Lindman, B. *Colloids Surf., A* **1997**, *129*, 3.
- (17) Valls, T.; Farrell, J. E. *Phys. Rev. E* **1993**, *47*, R36.
- (18) Kawakatsu, T.; Kawasaki, K.; Furusaka, M.; Okabayashi, H.; Kanaya, T. *J. Chem. Phys.* **1993**, *99*, 8200.
- (19) Shinozaki, A.; Oono, Y. *Phys. Rev. E* **1993**, *48*, 2622.
- (20) Cross, M. C.; Hohenberg P. C. *Rev. Mod. Phys.* **1993**, *65*, 851.
- (21) Schmittmann, B.; Zia, R. K. P.; *Phase Transitions and Critical Phenomena*; Domb, C., Lebowitz, J., Eds.; Academic Press: London, 1994.
- (22) Malcolm, G. N.; Rowlinson, J. S. *Trans. Faraday Soc.* **1957**, *53*, 921.
- (23) Barber, M. N.; Ninham, B. W. *Random and Restricted Walks*; Gordon and Breach: New York, 1970.
- (24) Abe, A.; Mark, J. E. *J. Am. Chem. Soc.* **1976**, *98*, 6468.
- (25) Maurits, N. M.; Vlimmeren, B. A. C. V. *Phys. Rev. E* **1997**, *56*, 816.
- (26) Vlimmeren, B. A. C. V.; Fraaije, J. G. E. M. *Comput. Phys. Commun.* **1996**, *99*, 21.
- (27) Barton, A. F. M. *Handbook of Solubility Parameters and Other Cohesion Parameters*; CRC Press: Boca Raton, FL, 1983.
- (28) Krevelen, D. W. *Properties of Polymers: Their Correlation with Chemical Structure, Their Numerical Estimation and Prediction from Additive Group Contributions*, 3rd ed.; Elsevier: Amsterdam, 1990.
- (29) Vlimmeren, B. A. C. V.; Maurits, N. M.; Zvelindovsky, A. V.; Fraaije, J. G. E. M. *Macromolecules* **1999**, *32*, 646.
- (30) Mays, H.; Almgren, M. *J. Phys. Chem. B* **1999**, *103*, 9432.
- (31) Guo, C.; Liu, H.-Z. *Colloids Surf., A* **2000**, *175*, 193.
- (32) Nagarajan, R. *Colloids Surf. B* **1999**, *16*, 55.
- (33) Nagarajan, R.; Ganesh, K. *Macromolecules* **1989**, *22*, 4312.
- (34) Alexandridis, P.; Andersson, K. *J. Colloid Interface Sci.* **1997**, *194*, 166.